Mathematical Biosciences and Engineering

https://www.aimspress.com/journal/mbe

MBE, 22(7): 1722–1750.
DOI: 10.3934/mbe.2025063
Received: 06 March 2025
Revised: 19 April 2025
Accepted: 12 May 2025
Published: 28 May 2025

Research article

Modeling the impact of temperature on the dynamics of carrier-dependent infectious diseases with control strategies

Shubham Chaudhry[1], Gauri Agrawal [2], Maia Martcheva[3] and A. K. Misra[4,*]

[1] Department of Mathematics, PPN College, CSJM University, Kanpur 208001, U.P., India

[2] Amity School of Applied Sciences, Amity University Uttar Pradesh, Lucknow Campus, Lucknow 226028, U.P., India

[3] Department of Mathematics, University of Florida, Gainesville 32611, USA

[4] Department of Mathematics, Institute of Science, Banaras Hindu University, Varanasi 221005, U.P., India

* **Correspondence:** Email: akmisra@bhu.ac.in.

Abstract: The spread of diseases poses significant threats to human health globally. The dynamic nature of infectious diseases, especially those that also rely on carriers (e.g., house flies) for transmission, requires innovative strategies to control their spread, as environmental conditions such as temperature, humidity, etc., affect the rate of growth of the carrier population. This study introduces a mathematical model to assess the effect of increasing global average temperature rise caused by carbon dioxide emissions and chemical control strategies on the dynamics of such diseases. The stability properties of feasible equilibrium solutions were discussed. Sensitivity analysis was also performed to highlight the key parameters that may help to design effective intervention strategies to control disease transmission. The model was further analyzed for an optimal control problem by incorporating a control measure on the application rate of chemical insecticides to reduce the carrier population. Through the combination of analytical techniques and numerical simulations, we have evaluated the effectiveness of chemical control strategies under varying epidemiological parameters. The model also explored the critical thresholds necessary for achieving disease control and eradication. Our results are valuable to public health officials and policymakers in designing effective interventions against carrier-dependent infectious diseases.

Keywords: mathematical model; carrier population; temperature rise; stability analysis; optimal control

1. Introduction

Over recent decades, the emergence of infectious diseases has increased significantly, posing serious threats to human health, worldwide. Some diseases spread in humans through the direct contact between susceptible and infected individuals [1]. However, certain diseases, like Typhoid fever, Salmonellosis, etc., spread in humans through carriers, like houseflies, apart from direct contact between susceptible and infected individuals. This is because of the fact that carriers transfer the pathogens of the diseases from contaminated sources to the edibles of humans, thus contaminating them. Due to the uptake of these contaminated edibles, individuals acquire the infection and make the disease more endemic in several regions of the world [2]. Research studies indicate that the increasing population density, healthcare disparities, global climate change, and the adaptive evolution of pathogens are the key factors for the emergence and proliferation of infectious diseases globally. These factors act synergistically to enhance disease transmission, promote the survival and spread of pathogens, and exacerbate the persistence of infectious diseases across diverse populations and regions [3, 4].

The correlation between the growth rate of the carrier population and temperature rise is studied by some researchers and it is pointed out that temperature rise attributes to the reproduction process of carriers and thus increases the density of carriers [5]. Over recent decades, the global atmospheric carbon dioxide (CO_2) level has been increasing due to anthropogenic activities, like urbanization, combustion of fossil fuels, deforestation, industrialization, etc., and is expected to continue rising [6]. It is noted that the global average temperature has also increased and is continuing to increase, but it was nearly constant before the pre-industrialization era [7]. The rise in this global average surface temperature is directly associated with the rising level of atmospheric carbon dioxide. Numerous research studies have highlighted that increasing carbon dioxide and temperature significantly contribute to the population density of vectors responsible for transmitting infectious diseases [8–10]. The elevated temperature creates favorable biological and ecological conditions for the growth of carriers, like houseflies [11, 12]. Higher temperature accelerates the metabolic processes of carriers, leading to faster development through their lifecycle phases (egg, larva, pupa, and adult). Eggs and larvae are less likely to perish in warmer conditions, ensuring higher survival rates and larger population [13, 14]. Global warming has also facilitated the expansion of vector habitats into regions previously restricted by colder climates. This geographical spread, combined with longer breeding seasons and improved survival rates, underscores the role of global average temperature rise in amplifying the ecological and epidemiological impact of vectors [15, 16].

Carrier-dependent diseases are significant contributors to localized outbreaks, resulting in considerable morbidity and mortality worldwide. The implementation of an effective vector (carrier) control strategy contributes in mitigating the transmission of these diseases. Such measures reduce the incidence of infections, thereby minimizing the risk of widespread epidemics. The application of insecticides is one of the most effective strategies to control vectors, provided it is utilized appropriately [17, 18]. Studies indicate that insecticides can be highly effective in vector control if used at the appropriate time and in an appropriate amount. The development of a vector, such as a housefly, typically takes about 7 to 10 days from egg to adult under favorable conditions, which include warm temperatures. Therefore, for the reduction of infectious diseases, the insecticides should be used during the vector's peak activity for optimal efficacy [19, 20]. Alongside this,

insufficient application of insecticides may fail to adequately control the vector population, thereby permitting their survival and continued transmission potential. Whereas, the overuse of insecticides to control the vectors increases the cost as well as possibly having damaging health outcomes for human beings. Thus, applying the correct amount of insecticides is crucial to control the vector population with minimum cost, which can be obtained by applying the insecticides in proportion to the vector population density [21].

During the past few decades, numerous mathematical models have been developed to capture the dynamics for the proliferation of infectious diseases and their possible control mechanisms, like vaccination, quarantine, medication, awareness, etc., and it is pointed out that these control mechanisms can halt the spread of diseases [22–29]. In recent past decades, the role of the carrier population on the disease transmission has also been studied by formulating mathematical models [30–33]. In particular, assuming that the carrier population follows logistic growth with an intrinsic growth rate and carrying capacity as a function of the human population, Singh et al. [34] analyzed a mathematical model and concluded that the presence of a carrier population renders the disease endemic in the considered region. To combat the transmission of carrier-dependent infectious diseases, Misra et al. [35] formulated and analyzed a mathematical model by assuming that the chemical insecticides are dispersed in proportion to the density of carriers in the considered region to reduce the density of the carrier population. They pointed out that the use of chemical insecticides is beneficial to reduce the infection in the region, but delay in spraying the chemical insecticides may lead to the destabilization of the system. As sprayed chemical insecticides may harm the human population and may be an economic burden on the government, therefore an optimal control problem is studied by Lata et al. [36] for optimal use of chemical insecticides to control the carrier population, and thus the disease.

As previously discussed, it is noted that an increase in the global average temperature significantly influences the proliferation of the carrier population, which may influence the transmission of infectious diseases among human beings. Therefore, in this study, we propose a mathematical model to assess the effect of global average temperature rise on carrier-dependent infectious diseases. We also aim to discuss a control strategy to reduce the carrier population as well as the proliferation of infectious diseases among the human population.

2. Mathematical model

We present a non-linear dynamical model by incorporating six variables and some non-negative parameters, with the aim of assessing their interactions based on certain assumptions. For this, we consider the dynamic variables, the concentrations of atmospheric CO_2 and global average temperature, and denote them as $C(t)$ and $T(t)$, respectively. Further, densities of total human population and carriers are represented as $N(t)$ and $F(t)$, respectively. Now, we divide the total human population into two subpopulations, such that $N(t) = S(t) + I(t)$. Here, $S(t)$ is the density of susceptible individuals, who are at risk of contracting the infectious disease, and $I(t)$ are those who are already infected and capable of spreading the infectious disease. Along with this, the variable $P(t)$ represents the concentration of sprayed chemical insecticides to control the population density of carriers.

In the process of modeling, we assume that the concentration of atmospheric carbon dioxide rises at a constant rate Q and it also increases at a rate μN due to anthropogenic activities. Since during

the pre-industrial era, the atmospheric level of CO_2 and the global average temperature were nearly constant, we represent the pre-industrial level of carbon dioxide by a constant C_0 and take the dilution rate coefficient as α_0. Thus, we incorporate the change in concentration of atmospheric CO_2 per unit time by $\alpha_0(C - C_0)$. Furthermore, it is observed that the increase in the atmospheric CO_2 also results to an increase in the level of global average temperature. Therefore, representing the pre-industrial level of global average temperature by a constant T_0, we assume that the global average temperature raises at a rate $\theta(C - C_0)$ and diminishes naturally at a rate $\theta_0(T - T_0)$, where θ and θ_0 represent the growth and depletion rate coefficients [37].

Proceeding further, it is assumed that the population density of susceptible individuals increases at a constant rate A, encompassing birth and immigration. The spread and proliferation of infectious disease is supposed to occur among the susceptible population primarily through two routes: direct contact between susceptible and infected persons and indirectly via carriers. Thus, we assume that the susceptible population gets infected at a rate βSI caused by direct interactions with the infected population, and indirectly due to the carrier population, and the susceptible population gets infected by consuming the carrier-induced contaminated edibles. In indirect transmission, we consider that the susceptible population transitions to the infected class in proportion to the density of the carrier population, having the disease transmission rate λ, by following a saturated-type functional response $\lambda SF/(m + F)$. Here, m represents a half saturation constant as the disease transmission rate becomes half when F reaches to m. Further, the densities of susceptible and infected individuals are assumed to be diminished due to natural mortality at a rate dS and dI, respectively; and the density of infected individuals is also reduced by disease-induced mortality at a rate αI. Since individuals recovering from carrier-dependent diseases do not obtain lifelong immunity and remain susceptible to reinfection, therefore, we place the recovered individuals from the infected to the susceptible class with the recovery rate νI.

Further, the growth rate of the carrier population is supposed to follow a logistic growth equation governed by

$$\frac{dF}{dt} = r_0 F\left(1 - \frac{F}{K_0}\right),$$

where r_0 represents the intrinsic growth rate, and K_0 is the carrying capacity of the carrier population. It is observed that temperature, humidity, precipitation, ecological changes, etc., all are crucial factors that affect the growth of the carrier population and thus the disease transmission; however, temperature significantly moderates the birth and growth of carriers. In the modeling phenomenon, we explicitly consider the global average temperature (T), which is caused by global carbon dioxide emissions (C). Though other factors like humidity, precipitation, and ecological changes also play an important role, to ensure clear, specific, and meaningful results, we focus on studying only one factor, i.e., temperature. It is noticed that warmer temperature provides more favorable environmental conditions for carriers to grow and enhance their population, which leads to a larger carrier population. Thus, we assume that $r(T)$ is the per-capita growth rate of the carrier population, which increases with the change in the global average temperature (T) such that $r(0) = r_0 > 0$ and $\frac{dr}{dT} > 0$. Also, $K(T)$ is considered to be the carrying capacity of the carrier population, affected by the global average temperature such that $K(0) = K_0 > 0$ and $\frac{dK}{dT} > 0$. Thus, the modified change in the growth rate of the carrier population is

considered as

$$\frac{dF}{dt} = r(T)F - r_0\frac{F^2}{K(T)}.$$

Moreover, it is observed that the haphazard disposal of garbage by humans contributes to the proliferation of carrier habitats. Therefore, we consider that the density of the carrier population increases at a rate ϕNF due to anthropogenic activities. Also, carrier population density naturally decreases because of unfavorable environmental conditions at a rate $\phi_0 F$. To control the carriers, chemical insecticides are assumed to be sprayed in the habitat of carriers in proportion to the density of the carrier population at a rate $\mu_2 F$. It is also assumed that the concentration of chemical insecticides naturally depletes at a rate $\mu_0 P$. The concentration of chemical insecticides depletes at a rate $\mu_1 PF$ because of its uptake by the carriers, and due to the absorption by carriers, their population density decreases in proportion to the uptake of chemical insecticides at a rate $\pi_1\mu_1 PF$.

Thus, the proposed model system is given by:

$$\begin{aligned}
\frac{dC}{dt} &= Q - \alpha_0(C - C_0) + \mu N,\\
\frac{dT}{dt} &= \theta(C - C_0) - \theta_0(T - T_0),\\
\frac{dS}{dt} &= A - \beta S I - \lambda S\frac{F}{m+F} + \nu I - dS,\\
\frac{dI}{dt} &= \beta S I + \lambda S\frac{F}{m+F} - (\nu + \alpha + d)I,\\
\frac{dF}{dt} &= r(T)F - r_0\frac{F^2}{K(T)} + \phi NF - \phi_0 F - \pi_1\mu_1 PF,\\
\frac{dP}{dt} &= \mu_2 F - \mu_0 P - \mu_1 PF,
\end{aligned} \tag{2.1}$$

having initial conditions $C(0) \geq C_0,\ T(0) \geq T_0,\ S(0) > 0,\ I(0) \geq 0,\ F(0) \geq 0,\ P(0) \geq 0$.

Now, in order to analyze model system (2.1), we consider $S + I = N$ and rewrite the above model system as the following model system:

$$\begin{aligned}
\frac{dC}{dt} &= Q - \alpha_0(C - C_0) + \mu N,\\
\frac{dT}{dt} &= \theta(C - C_0) - \theta_0(T - T_0),\\
\frac{dN}{dt} &= A - dN - \alpha I,\\
\frac{dI}{dt} &= \beta(N - I)I + \lambda(N - I)\frac{F}{m+F} - (\nu + \alpha + d)I,\\
\frac{dF}{dt} &= r(T)F - r_0\frac{F^2}{K(T)} + \phi NF - \phi_0 F - \pi_1\mu_1 PF,\\
\frac{dP}{dt} &= \mu_2 F - \mu_0 P - \mu_1 PF,
\end{aligned} \tag{2.2}$$

having initial conditions $C(0) \geq C_0,\ T(0) \geq T_0,\ N(0) > 0,\ I(0) \geq 0,\ F(0) \geq 0,\ P(0) \geq 0$.

Lemma 1. *The bounded set, containing the region of attraction for model system* (2.2)*, which attracts all solutions to the interior of the positive orthant, is given as:*

$$\Omega = \Bigg\{(C, T, N, I, F, P) \in \mathbb{R}^6_+ : C_0 \le C \le C_m, T_0 \le T \le T_m, 0 \le I \le N \le \frac{A}{d},$$
$$0 \le F \le F_m, 0 \le P \le \frac{\mu_2 F_m}{\mu_0}\Bigg\},$$

where $C_m = C_0 + \frac{1}{\alpha_0}\left(Q + \frac{\mu A}{d}\right)$, $T_m = T_0 + \frac{\theta}{\theta_0\alpha_0}\left(Q + \frac{\mu A}{d}\right)$, *and* $F_m = \frac{K(T_m)}{r_0}\left\{r(T_m) + \frac{\phi A}{d} - \phi_0\right\}$. *Here,* $\left(r(T_m) + \frac{\phi A}{d} - \phi_0\right)$ *is assumed to be positive. The proof can be followed by [38, 39].*

3. Feasibility of equilibrium points

We determine the equilibrium points of model system (2.2) by nullifying the time derivative of all dynamic variables. Results of the analyzed equilibria are summarized in the below-mentioned theorem.

Theorem 1. *For the model system* (2.2)*, three non-negative equilibria exist:*

- *Disease-free equilibrium (DFE),* $E_0(\overline{C}, \overline{T}, \frac{A}{d}, 0, 0, 0)$. *Here,* $\overline{C} = C_0 + \frac{1}{\alpha_0}(Q + \mu\frac{A}{d})$ *and* $\overline{T} = T_0 + \frac{\theta}{\alpha_0\theta_0}\left(Q + \mu\frac{A}{d}\right)$.
- *Carrier-free equilibrium (CFE)* $E_1(\hat{C}, \hat{T}, \hat{N}, \hat{I}, 0, 0)$*, where* $\hat{C} = C_0 + \dfrac{Q}{\alpha_0} + \dfrac{\mu\left(\beta A + \alpha(\nu + \alpha + d)\right)}{\alpha_0\beta(\alpha + d)}$, $\hat{T} = T_0 + \dfrac{\theta Q}{\alpha_0\theta_0} + \dfrac{\theta\mu\left(\beta A + \alpha(\nu + \alpha + d)\right)}{\alpha_0\theta_0\beta(\alpha + d)}$, $\hat{N} = \dfrac{\beta A + \alpha(\nu + \alpha + d)}{\beta(\alpha + d)}$, $\hat{I} = \dfrac{\beta A - (\nu + \alpha + d)d}{\beta(\alpha + d)}$. *This equilibrium is feasible if the basic reproduction number* $R_0 = \dfrac{\beta A}{d(\nu + \alpha + d)} > 1$.
- *Interior equilibrium* $E^*(C^*, T^*, N^*, I^*, F^*, P^*)$ *exists provided* $F_0 > 0$*, where* F_0 *is defined in the proof.*

Proof. The existence of all three equilibria can be determined by analyzing the following set of equations. For simplicity, we keep the same variables with different symbols, using the overline, hat, and asterisk to distinguish the carrier-free, disease-free, and interior equilibrium points, respectively.

$$Q - \alpha_0(C - C_0) + \mu N = 0, \tag{3.1}$$
$$\theta(C - C_0) - \theta_0(T - T_0) = 0, \tag{3.2}$$
$$A - dN - \alpha I = 0, \tag{3.3}$$
$$\beta(N - I)I + \lambda(N - I)\frac{F}{m + F} - (\nu + \alpha + d)I = 0, \tag{3.4}$$
$$r(T)F - r_0\frac{F^2}{K(T)} + \phi NF - \phi_0 F - \pi_1\mu_1 PF = 0, \tag{3.5}$$
$$\mu_2 F - \mu_0 P - \mu_1 PF = 0. \tag{3.6}$$

Since it is readily apparent that the disease-free equilibrium $E_0(\overline{C}, \overline{T}, \frac{A}{d}, 0, 0, 0)$ exists, the proof is omitted. Now, the proofs for the existence of carrier-free equilibrium $E_1(\hat{C}, \hat{T}, \hat{N}, \hat{I}, 0, 0)$ and interior equilibrium $E^*(C^*, T^*, N^*, I^*, F^*, P^*)$ are as follows:

3.1. Feasibility of carrier-free equilibrium (CFE) $E_1(\hat{C}, \hat{T}, \hat{N}, \hat{I}, 0, 0)$

For the case when $F = 0$, $P = 0$, and $I \neq 0$, from Eq (3.4), we have

$$\beta(N - I) - (\nu + \alpha + d) = 0. \tag{3.7}$$

By Eq (3.3), we have

$$I = \frac{A - dN}{\alpha}. \tag{3.8}$$

Thus, using Eq (3.8) in (3.7), we get

$$N = \frac{A}{\alpha + d} + \frac{\alpha(\nu + \alpha + d)}{\beta(\alpha + d)} = \frac{\beta A + \alpha(\nu + \alpha + d)}{\beta(\alpha + d)} =: \hat{N}. \tag{3.9}$$

Thus, from Eqs (3.8) and (3.9), we obtain

$$I = \frac{A - d\hat{N}}{\alpha} = \frac{\beta A - (\nu + \alpha + d)d}{\beta(\alpha + d)} =: \hat{I}, \tag{3.10}$$

which is positive if $\beta A - d(\nu + \alpha + d)$ is greater than zero, i.e., $R_0 = \dfrac{\beta A}{d(\nu + \alpha + d)} > 1$.
Further, using Eqs (3.1) and (3.2), we get

$$C = C_0 + \frac{Q}{\alpha_0} + \frac{\mu(\beta A + \alpha(\nu + \alpha + d))}{\alpha_0\beta(\alpha + d)} =: \hat{C}$$

and

$$T = T_0 + \frac{\theta Q}{\alpha_0\theta_0} + \frac{\theta\mu(\beta A + \alpha(\nu + \alpha + d))}{\alpha_0\theta_0\beta(\alpha + d)} =: \hat{T}.$$

Hence, CFE equilibrium $E_1(\hat{C}, \hat{T}, \hat{N}, \hat{I}, 0, 0)$ exists only when $R_0 > 1$.

3.2. Feasibility of interior equilibrium $E^*(C^*, T^*, N^*, I^*, F^*, P^*)$

Using Eqs (3.1) and (3.3) in Eq (3.2), we obtain the variable T as a function of I, given as

$$T = T_0 + \frac{\theta Q}{\alpha_0\theta_0} + \frac{\theta\mu(A - \alpha I)}{d\alpha_0\theta_0} = f(I). \tag{3.11}$$

Now, putting Eq (3.11) into Eq (3.5), we obtain an equation involving both the variables I and F, and denote it by $H(I, F)$ as follows:

$$H(I, F) = r(f(I)) - r_0\frac{F}{K(f(I))} + \frac{(A - \alpha I)\phi}{d} - \pi_1\mu_1\mu_2\frac{F}{(\mu_0 + \mu_1 F)} - \phi_0 = 0. \tag{3.12}$$

Differentiating the function $H(I, F)$ partially with respect to F, we get

$$\frac{\partial H}{\partial F} = -\frac{r_0}{K(f(I))} - \frac{\pi_1\mu_1\mu_2\mu_0}{(\mu_0 + \mu_1 F)^2} \neq 0, \forall\, I \in \left(0, \frac{A}{\alpha}\right), \tag{3.13}$$

because the parameters $r_0,\ \pi_1,\ \mu_1,\ \mu_2,\ \mu_0$ are non-zero. Thus, by the implicit function theorem, we can write $F = g(I),\ \forall\, I \in \left(0, \frac{A}{\alpha}\right)$. By Eq (3.12), we can observe that the function $H(I, F)$ is a decreasing

function of F for every fixed I. Thus, for every fixed value of I, if a solution exists, it is unique. That defines $F = g(I)$. Here, it is worth noting that the functions $f(I)$ and $g(I)$ are defined for $I \in \left(0, \frac{A}{\alpha}\right)$. Here, it may also be noted that we always have a unique positive value of F (say F_0) for $I = 0$ if and only if

$$r(f(0)) + \frac{A\phi}{d} - \phi_0 > 0. \tag{3.14}$$

Here, F_0 is the unique positive solution of $H(0, F) = 0$, which yields a quadratic equation and provides a positive value F_0 under the necessary and sufficient condition (3.14).

Proceeding further, using Eqs (3.3) and (3.4), and substituting $F = g(I)$, we derive an equation in the variable I and denote it by $G(I)$ as:

$$G(I) = \beta\left\{\frac{A - (\alpha + d)I}{d}\right\} I + \lambda\left\{\frac{A - (\alpha + d)I}{d}\right\} \frac{g(I)}{m + g(I)} - (\nu + \alpha + d)I = 0. \tag{3.15}$$

From (3.15), we may note that

$$G(0) = \frac{\lambda A F_0}{d(m + F_0)} > 0, \text{ and } G\left(\frac{A}{\alpha + d}\right) = -\frac{(\nu + \alpha + d)A}{(\alpha + d)} < 0. \tag{3.16}$$

To show the uniqueness of the obtained positive root, first we differentiate the function $G(I)$ with respect to I and get

$$G'(I) = \beta\left\{\frac{A - (\alpha + d)I}{d}\right\} - (\nu + \alpha + d) - \frac{\beta(\alpha + d)}{d} I - \frac{\lambda(\alpha + d)g(I)}{d(m + g(I))} + \lambda m\left\{\frac{A - (\alpha + d)I}{d}\right\} \frac{g'(I)}{(m + g(I))^2}. \tag{3.17}$$

Since $\frac{dF}{dI} = g'(I) < 0$, this implies that $G'(I) < 0$ for I^*. Now, let us assume the contrary that there exist two distinct roots $I_1^* \neq I_2^*$, such that $G(I_1^*) = G(I_2^*) = 0$. If both the roots I_1^* and I_2^* are of odd multiplicity (in particular, one), then $G(0) > 0$, $G(I_1^*) = 0$, $G\left(\frac{I_1^* + I_2^*}{2}\right) < 0$, $G(I_2^*) = 0$, and $G\left(\frac{A}{\alpha+d}\right) > 0$. The last inequality contradicts the fact that $G\left(\frac{A}{\alpha+d}\right) < 0$ as shown in (3.16). Hence, one of I_1^* and I_2^* has an even multiplicity (say, 2). Then, we may assume that I_1^* has multiplicity two, and then $G'(I_1^*) = 0$. But, according to Eq (3.17), $G'(I_1^*) < 0$. Hence, this is a contradiction.

Further, let us assume that there exist three distinct roots $I_1^* \neq I_2^* \neq I_3^*$, and they all must be of odd multiplicity, so that $G\left(\frac{A}{\alpha+d}\right) < 0$. But, according to Eq (3.17), $G'(I_j^*) < 0$; $i = 1, 2, 3$, and this is impossible as $G(I)$ must be increasing at one of these three intersections. Hence, multiple solutions of $G(I)$ are not possible. Thus, Eq (3.15) has a unique solution I^* in the interval $\left(0, \frac{A}{\alpha+d}\right)$ if and only if $\left(r(f(0)) + \frac{A\phi}{d} - \phi_0\right) > 0$. Thus, using this unique positive value of I^*, we obtain the unique positive values of C^*, T^*, N^*, F^*, and P^*. Hence, the interior equilibrium (E^*) exists.

Remark 1. *The analytical results show that* $\frac{dI^*}{d\mu} > 0$, $\frac{dF^*}{d\mu} > 0$, $\frac{dI^*}{d\theta} > 0$, *and* $\frac{dF^*}{d\theta} > 0$. *These findings highlight that an increase in the emission rate of carbon dioxide due to human activities leads to enhance the density of infected individuals as well as the density of carriers. Additionally, the findings* $\frac{dI^*}{d\phi} > 0$ *and* $\frac{dF^*}{d\phi} > 0$ *depict that as the density of carriers caused by human-driven activities increases, the densities of infected persons as well as carriers both increase. Thus, these findings suggest a direct correlation between carbon dioxide emissions and infectious disease transmission. The environmental changes, like global warming or altered ecosystems, may create conditions more favorable for the proliferation of the carrier population, and thus may increase the endemicity of disease.*

4. Local stability analysis

To analyze the local stability of DFE and CFE, we evaluate the Jacobian matrix for our model (2.2) at the corresponding equilibrium points, i.e., E_0 and E_1, and examine the sign of the real parts of the roots of the obtained characteristic equation. For this, we have the matrix $J(E)$ for system (2.2) as

$$J(E) = \begin{bmatrix} -\alpha_0 & 0 & \mu & 0 & 0 & 0 \\ \theta & -\theta_0 & 0 & 0 & 0 & 0 \\ 0 & 0 & -d & -\alpha & 0 & 0 \\ 0 & 0 & a_{43} & a_{44} & a_{45} & 0 \\ 0 & a_{52} & \phi F & 0 & a_{55} & -\pi_1\mu_1 F \\ 0 & 0 & 0 & 0 & (\mu_2 - \mu_1 P) & -(\mu_0 + \mu_1 F) \end{bmatrix},$$

where

$$a_{43} = \beta I + \lambda\frac{F}{m+F},\ a_{44} = \beta(N-2I) - \lambda\frac{F}{m+F} - (\nu+\alpha+d),\ a_{45} = \lambda(N-I)\frac{m}{(m+F)^2},$$

$$a_{52} = r'(T)F + r_0\frac{F^2K'(T)}{(K(T))^2},\ a_{55} = r(T) - 2r_0\frac{F}{K(T)} + \phi N - \phi_0 - \pi_1\mu_1 P.$$

Now, on evaluating the matrix $J(E)$ at DFE $E_0(\overline{C}, \overline{T}, \frac{A}{d}, 0, 0, 0)$, we get four negative eigenvalues given as $-\alpha_0$, $-\theta_0$, $-\mu_0$, $-d$, and the other two eigenvalues are obtained as $r(\overline{T}) + \phi\frac{A}{d} - \phi_0$ and $\beta\frac{A}{d} - (\nu + \alpha + d)$. Here, it may be noted that the eigenvalue $\beta\frac{A}{d} - (\nu+\alpha+d)$ can be written as $(\nu + \alpha + d)(R_0 - 1)$, which is positive (or negative) for $R_0 > 1$ (or $R_0 < 1$). Thus, DFE $E_0(\overline{C}, \overline{T}, \frac{A}{d}, 0, 0, 0)$ is stable only when $r(\overline{T}) + \phi\frac{A}{d} - \phi_0 < 0$ and $R_0 < 1$. Further, the analysis of the evaluated Jacobian matrix, corresponding to CFE $E_1(\hat{C}, \hat{T}, \hat{N}, \hat{I}, 0, 0)$ reveals that one of the eigenvalues $r(\hat{T}) + \phi\hat{N} - \phi_0 > 0$ if the interior equilibrium E^* exists. Thus, CFE E_1 is unstable if E^* exists. The results for the local stability of DFE and CFE are summarized in the following theorem.

Theorem 2. *(i). The disease-free equilibrium* $E_0(\overline{C}, \overline{T}, \frac{A}{d}, 0, 0, 0)$ *is stable only when* $r(\overline{T}) + \phi\frac{A}{d} - \phi_0 < 0$ *and* $R_0 < 1$.
(ii). The carrier-free equilibrium $E_1(\hat{C}, \hat{T}, \hat{N}, \hat{I}, 0, 0)$ *is stable if* $r(\hat{T}) + \phi\hat{N} - \phi_0 < 0$.

The given theorem provides conditions for the stability of the DFE and CFE of the epidemiological model (2.2). Practically, the DFE implies that the system will tend to eliminate the disease and maintain a state free of infectious disease if the two mentioned criteria are satisfied for its stability. First, the intrinsic growth rate of the carrier population ($r(\bar{T})$) and the increase in carriers due to the anthropogenic activities $\left(\phi\frac{A}{d}\right)$ collectively must not exceed the natural depletion rate of the density of carriers because of unfavorable environmental conditions (ϕ_0). Also, the basic reproduction number being less than unity indicates that, on average, an infected individual transmits the disease to fewer than one person. This theorem underscores the importance of reducing R_0 through public health interventions and controlling factors contributing to disease spread. Further, the stability of the carrier-free equilibrium $E_1(\hat{C}, \hat{T}, \hat{N}, \hat{I}, 0, 0)$ indicates that the system will eliminate the carrier population while allowing other components of the system to persist in a balanced state. The condition $r(\hat{T}) + \phi\hat{N} - \phi_0 < 0$ implies that the intrinsic growth rate of carriers, $r(\hat{T})$ combined with

the increment in carrier population due to anthropogenic activities ($\phi\hat{N}$), must be less than the natural depletion rate of carriers resulting from unfavorable environmental factors (ϕ_0). In this condition, carriers cannot sustain their population, which is crucial in breaking the transmission cycle of carrier-dependent infectious diseases. From a practical perspective, it emphasizes the importance of controlling environmental and anthropogenic factors that promote carrier proliferation to achieve a stable carrier-free equilibrium.

Proceeding further, we present the following theorem and its proof using Lyapunov's stability theory regarding the local stability behavior of interior equilibrium [40].

Theorem 3. *The interior equilibrium $E^*(C^*, T^*, N^*, I^*, F^*, P^*)$ exhibits the local asymptotic stability provided the underlying inequalities are satisfied:*

$$3\alpha\lambda^2 F^{*2} < 2\beta^2 dI^{*2}(m + F^*)^2, \tag{4.1}$$

$$\frac{27\alpha\lambda^2(N^* - I^*)^2 m^2}{8(m + F^*)^4} < \frac{r_0^2\beta^2 dI^{*2}}{\phi^2(K(T^*))^2}, \tag{4.2}$$

$$\frac{\alpha(\mu_2 - \mu_1 P^*)K(T^*)}{\pi_1\mu_1} < \frac{4\alpha_0^2\theta_0^2 r_0\beta d}{9\mu^2\theta^2\left\{r'(T^*) + \frac{r_0K'(T^*)F^*}{(K(T^*))^2}\right\}^2}. \tag{4.3}$$

Proof. Let us consider the small perturbations around the interior equilibrium $E^*(C^*, T^*, N^*, I^*, F^*, P^*)$ as

$$C = \tilde{c} + C^*,\ \ T = \tilde{t_s} + T^*,\ \ N = \tilde{n} + N^*,\ \ I = \tilde{i} + I^*,\ \ F = \tilde{f} + F^*,\ \ P = \tilde{p} + P^*,$$

and define a function

$$V = \frac{m_0}{2}\tilde{c}^2 + \frac{m_1}{2}\tilde{t_s}^2 + \frac{m_2}{2}\tilde{n}^2 + \frac{m_3}{2}\tilde{i}^2 + \frac{m_4}{2}\tilde{f}^2 + \frac{m_5}{2}\tilde{p}^2, \tag{4.4}$$

where the constants $m_i's, i = 0, 1, ..., 5$, have arbitrary positive values. Now, we get the time derivative of the function V along a linearized solution of system (2.2) as

$$\begin{aligned}\frac{dV}{dt} =& -m_3\left\{\frac{\lambda F^*N^*}{(m + F^*)I^*}\right\}\tilde{i}^2 - m_5(\mu_0 + \mu_1 F^*)\tilde{p}^2 - m_0\alpha_0\tilde{c}^2 - m_1\theta_0\tilde{t_s}^2 - m_2 d\tilde{n}^2 - m_3\beta I^*\tilde{i}^2\\ &- m_4 r_0\frac{F^*}{K(T^*)}\tilde{f}^2 + m_3\left(\frac{\lambda F^*}{m + F^*}\right)\tilde{n}\tilde{i} + m_3\lambda(N^* - I^*)\frac{m}{(m + F^*)^2}\tilde{i}\tilde{f} + (m_0\mu)nc + (m_1\theta)\tilde{c}\tilde{t_s}\\ &+ m_4\left\{r'(T^*)F^* + \frac{r_0K'(T^*)F^{*2}}{(K(T^*))^2}\right\}\tilde{t_s}\tilde{f} + (m_4\phi F^*)\tilde{n}\tilde{f} + \{m_5(\mu_2 - \mu_1 P^*) - m_4\pi_1\mu_1 F^*\}\tilde{p}\tilde{f}\\ &+ (m_3\beta I^* - m_2\alpha)\tilde{n}\tilde{i}.\end{aligned} \tag{4.5}$$

Now, on choosing the constants $m_2 = \frac{\beta}{\alpha}$, $m_3 = \frac{1}{I^*}$, $m_4 = \frac{(\mu_2 - \mu_1 P^*)}{\pi_1\mu_1 F^*}$ and $m_5 = 1$, $\frac{dV}{dt}$ remains negative definite provided the underlying inequalities hold:

$$3\alpha\lambda^2 F^{*2} < 2\beta^2 dI^{*2}(m + F^*)^2, \tag{4.6}$$

$$\alpha m_0 < \frac{2\alpha_0 d\beta}{3\mu^2}, \tag{4.7}$$

$$m_1 < \frac{\alpha_0\theta_0}{\theta^2}m_0, \tag{4.8}$$

$$\frac{\lambda^2(N^*-I^*)^2m^2K(T^*)}{r_0\beta I^{*2}(m+F^*)^4} < \frac{2(\mu_2-\mu_1P^*)}{3\pi_1\mu_1}, \tag{4.9}$$

$$\frac{\alpha(\mu_2-\mu_1P^*)}{\pi_1\mu_1} < \frac{4\beta d r_0}{9K(T^*)\phi^2}, \tag{4.10}$$

$$\frac{4(\mu_2-\mu_1P^*)}{9\pi_1\mu_1} < \frac{2r_0\theta_0m_1}{3K(T^*)\left\{r'(T^*)+\frac{r_0K'(T^*)F^*}{(K(T^*))^2}\right\}^2}. \tag{4.11}$$

Using the inequalities (4.7), (4.8), and (4.11), we get

$$\frac{\alpha(\mu_2-\mu_1P^*)}{\pi_1\mu_1} < \frac{4r_0\theta_0^2\alpha_0^2d\beta}{9\mu^2\theta^2K(T^*)\left\{r'(T^*)+\frac{r_0K'(T^*)F^*}{(K(T^*))^2}\right\}^2}. \tag{4.12}$$

The inequalities (4.9) and (4.10) reduce to

$$\frac{27\alpha\lambda^2(N^*-I^*)^2m^2}{8(m+F^*)^4} < \frac{r_0^2\beta^2dI^{*2}}{\phi^2(K(T^*))^2}. \tag{4.13}$$

Thus, E^* exhibits the local asymptotic stability under the conditions (4.6), (4.12), and (4.13).

Remark 2. *For $\alpha = 0$, we noticed that $N^* = A/d$, which is a fixed value. It clearly says that the equilibrium value of N^*, i.e., the sum of susceptible and infected individuals, will always be constant irrespective of infection in the community. In this case, the interior equilibrium, if it exists, will always be stable and the endemicity of disease will be independent of other parameters.*

The local asymptotic stability of the interior equilibrium is contingent on satisfying a set of inequalities that collectively govern the interplay between disease dynamics, environmental conditions, and anthropogenic influences. The obtained inequalities define the thresholds and conditions under which the interior equilibrium remains locally stable. Practically, this means that disease persistence and coexistence of infected and carrier populations are possible but require finely tuned ecological and epidemiological parameters to prevent instability. This analysis underscores the importance of managing resources, reducing anthropogenic pressures, and controlling transmission–related factors to achieve stability in complex disease ecosystems.

5. Global stability analysis

We analyze the global stability of equilibrium E^* by employing Lyapunov's direct method [41, 42] and provide the underlying theorem.

Theorem 4. *With the consideration that $r(T)$ satisfies $0 \le r'(T) \le p$ for a positive constant p, and $K(T)$ satisfies $0 \le K'(T) \le q$ for a positive constant q, the interior equilibrium E^* exhibits the*

global asymptotic stability behavior inside the region of attraction Ω *provided the underlying inequalities hold:*

$$3\alpha\lambda^2 < 2\beta^2 dI^{*2}, \tag{5.1}$$

$$\alpha(\mu_2 - \mu_1 P^*)\phi^2 < \frac{4\beta d r_0}{9K(T^*)}, \tag{5.2}$$

$$\frac{\lambda^2 m^2 (N^* - I^*)^2}{(m + F^*)^2 (m + F_m)^2 I^{*2}} < \frac{2(\mu_2 - \mu_1 P^*) r_0 \beta}{3K(T^*)}, \tag{5.3}$$

$$\alpha(\mu_2 - \mu_1 P^*) < \frac{4\alpha_0^2 \theta_0^2 r_0 d\beta}{9\theta^2 \mu^2 K(T^*) \left\{ p + r_0 F_m \frac{q}{K_0^2} \right\}^2}. \tag{5.4}$$

Here, F_m *represents the maximum value of the density of the carrier population.*

Proof. To prove the aforementioned theorem, we employ Lyapunov's direct method, and consider the following function:

$$\begin{aligned} W \;=\; & \frac{n_0}{2}(C - C^*)^2 + \frac{n_1}{2}(T - T^*)^2 + \frac{n_2}{2}(N - N^*)^2 + n_3 \left(I - I^* - I^* \ln \frac{I}{I^*} \right) \\ & + n_4 \left(F - F^* - F^* \ln \frac{F}{F^*} \right) + \frac{n_5}{2}(P - P^*)^2, \end{aligned} \tag{5.5}$$

where the constants $n_i' s, i = 0, 1, ..., 5$, have arbitrary positive values. Proceeding further, the differentiation of the function W given by Eq (5.5) with respect to time t, and some algebraic simplifications, yield that,

$$\begin{aligned} \frac{dW}{dt} = & -\left[\frac{n_0 \alpha_0}{2}(C - C^*)^2 - n_1 \theta (C - C^*)(T - T^*) + \frac{n_1 \theta_0}{2}(T - T^*)^2 \right] \\ & - \left[\frac{n_0 \alpha_0}{2}(C - C^*)^2 - n_0 \mu (C - C^*)(N - N^*) + \frac{n_2 d}{3}(N - N^*)^2 \right] \\ & - \left[\frac{n_2 d}{3}(N - N^*)^2 - n_3 \frac{\lambda F}{(m + F) I^*}(N - N^*)(I - I^*) + \frac{n_3 \beta}{2}(I - I^*)^2 \right] \\ & - \left[\frac{n_2 d}{3}(N - N^*)^2 - n_4 \phi (N - N^*)(F - F^*) + \frac{n_4 r_0}{3K(T^*)}(F - F^*)^2 \right] \\ & - \left[\frac{n_1 \theta_0}{2}(T - T^*)^2 - n_4 (f(T) + r_0 F g(T))(T - T^*)(F - F^*) + \frac{n_4 r_0}{3K(T^*)}(F - F^*)^2 \right] \\ & - \left[n_3 \frac{\beta}{2}(I - I^*)^2 - n_3 \frac{\lambda m (N^* - I^*)}{(m + F)(m + F^*) I^*}(I - I^*)(F - F^*) + \frac{n_4 r_0}{3K(T^*)}(F - F^*)^2 \right] \\ & - n_3 \left\{ \frac{\lambda N F}{(m + F) I I^*} \right\} (I - I^*)^2 + (n_3 \beta - n_2 \alpha)(N - N^*)(I - I^*) + \Big(n_5 (\mu_2 - \mu_1 P^*) \\ & - n_4 \pi_1 \mu_1 \Big)(F - F^*)(P - P^*) - n_5 (\mu_0 + \mu_1 F)(P - P^*)^2. \end{aligned} \tag{5.6}$$

Here, we specify $f(T)$ and $g(T)$ as a function of temperature T such that:

$$f(T) = \begin{cases} \dfrac{r(T) - r(T^*)}{T - T^*}, & T \neq T^*, \\ \dfrac{dr}{dT}, & T = T^*, \end{cases} \tag{5.7}$$

$$g(T) = \begin{cases} \dfrac{K(T) - K(T^*)}{T - T^*} . \dfrac{1}{K(T).K(T^*)}, & T \neq T^*, \\ \dfrac{1}{K^2(T^*)} . \dfrac{dK}{dT}, & T = T^*. \end{cases} \tag{5.8}$$

Now, with the consideration of this theorem, on applying the mean value theorem, the underlying results are obtained:

$$|f(T)| \leq p \quad \text{and} \quad |g(T)| \leq \frac{q}{K_0^2}. \tag{5.9}$$

Proceeding further, by employing Sylvester's criterion and choosing the constants $n_2 = \beta/\alpha$, $n_3 = 1$, $n_4 = (\mu_2 - \mu_1 P^*)$, and $n_5 = \pi_1\mu_1$, the derivative $\frac{dW}{dt}$ is negative definite provided the underlying inequalities hold:

$$n_1 < \frac{\alpha_0\theta_0}{\theta^2} n_0, \tag{5.10}$$

$$\alpha n_0 < \frac{2\alpha_0\beta d}{3\mu^2}, \tag{5.11}$$

$$3\alpha\lambda^2 < 2\beta^2 d I^{*2}, \tag{5.12}$$

$$(\mu_2 - \mu_1 P^*) < \frac{2r_0\theta_0 n_1}{3K(T^*)\left\{p + r_0 F_m \frac{q}{K_0^2}\right\}^2}, \tag{5.13}$$

$$\alpha(\mu_2 - \mu_1 P^*)\phi^2 < \frac{4\beta d r_0}{9K(T^*)}, \tag{5.14}$$

$$\frac{\lambda^2 m^2 (N^* - I^*)^2}{(m + F^*)^2 (m + F_m)^2 I^{*2}} < \frac{2(\mu_2 - \mu_1 P^*) r_0 \beta}{3K(T^*)}. \tag{5.15}$$

Using the inequalities (5.10), (5.11), and (5.13), we get

$$\alpha(\mu_2 - \mu_1 P^*) < \frac{4\alpha_0^2\theta_0^2 r_0 d\beta}{9\theta^2\mu^2 K(T^*)\left\{p + r_0 F_m \dfrac{q}{K_0^2}\right\}^2}, \tag{5.16}$$

where $F_m = \frac{K(T_m)}{r_0}\left\{r(T_m) + \frac{\phi A}{d} - \phi_0\right\}$, and thus, under the bounded set Ω, the equilibrium $E^*(C^*, T^*, N^*, I^*, F^*, P^*)$ shows the global asymptotic stability, provided the conditions (5.12), (5.14), (5.15), and (5.16) are satisfied.

6. Formulation of the optimal control problem

In the optimal control problem, we present a strategy to minimize the carrier population, along with the spraying rate of chemical insecticides. We focus on minimizing the carrier population since the carriers affect the susceptible individuals and infect them leading to the proliferation of the infectious disease. Therefore, to reduce the spread of carrier-dependent infections, we must focus on reducing the carriers through which the infection is proliferating. By the proposed model system, it can be seen that a reduction in the carrier population directly leads to a reduction in the number of infected individuals. To achieve this, we apply the optimal control measures, aiming at minimizing the carrier population through the use of chemical insecticides. In the present section, we devise a strategy to minimize the carrier population, along with the spraying rate of chemical insecticides. Here, the spraying rate coefficient μ_2 is treated as a Lebesgue measurable function over a finite time interval $[0, T_f]$, rather than a constant. As a result, μ_2 becomes a variable, denoted by $w(t)$. With this assumption, our objective is to minimize the total cost functional $J(w)$, allowing us to reformulate model system (2.2) accordingly.

$$\begin{aligned}
\frac{dC}{dt} &= Q - \alpha_0(C - C_0) + \mu N,\\
\frac{dT}{dt} &= \theta(C - C_0) - \theta_0(T - T_0),\\
\frac{dN}{dt} &= A - dN - \alpha I,\\
\frac{dI}{dt} &= \beta(N - I)I + \lambda(N - I)\frac{F}{m + F} - (\nu + \alpha + d)I,\\
\frac{dF}{dt} &= r(T)F - r_0\frac{F^2}{K(T)} + \phi NF - \phi_0 F - \pi_1\mu_1 PF,\\
\frac{dP}{dt} &= w(t)F - \mu_0 P - \mu_1 PF,
\end{aligned} \tag{6.1}$$

subject to the initial conditions $C(0) \geq C_0,\ T(0) \geq T_0,\ N(0) > 0,\ I(0) \geq 0,\ F(0) \geq 0,\ P(0) \geq 0.$

$$J(w) = \int_0^{T_f} [P_1 F(t) + Q_1 w^2(t)]dt. \tag{6.2}$$

In the cost functional, the constants P_1 and Q_1 represent positive weights that ensure the units of the integrands in $J(w)$ are balanced. The term $P_1 F(t)$ represents the costs incurred due to the epidemic and the carrier population, while $Q_1 w^2(t)$ reflects the expenses associated with the application of chemical insecticides to reduce carrier density [43–45]. Our objective is to determine the optimal control function w^* such that

$$J(w^*) = \min_{w \in U} J(w), \tag{6.3}$$

subject to (6.1), where U is the control set, and is defined as:

$$U = \left\{(w) : w \text{ is measurable}, 0 \leq w \leq w_{max} \text{ for } t \in [0, T_f]\right\}.$$

6.1. Existence of optimal control

Theorem 5. *There exists an optimal control $w^* \in U$ such that*

$$J(w^*) = \min_{w \in U} J(w), \tag{6.4}$$

subject to the system (6.1) *with initial conditions.*

Proof. The boundedness of the solution to system (6.1) confirms the existence of a valid control solution. Consequently, both the control variable and corresponding state variables are guaranteed to exist. Additionally, the convexity condition for the objective functional in $w(t)$ is satisfied. It is defined that the control set is characterized as both convex and closed, and there exist positive constants p_1, $p_2 > 0$, and $q > 1$ such that

$$P_1F(t) + Q_1w^2(t) \geq p_2(\mid w \mid)^q - p_1,$$

where p_1 and p_2 depend on $F(t)$ and Q_1, respectively. For details to assess the feasibility of the optimal control problem, follow the results from Lukes (Theorem 9.2.1, page 182) [46], and Fleming and Rishel (Theorem 4.1, pages 68 and 69) [47].

6.2. Characterization of optimal control

After defining the optimal control problem, the principle of optimal control, known as Pontryagin's maximum principle [48,49] is utilized to establish the necessary conditions for obtaining the optimal control strategy. This leads to the formulation of the Hamiltonian function, which represents the dynamics and cost structure of the control problem:

$$\begin{aligned} H(C,T,N,I,F,P,w,\zeta_1,\zeta_2,\zeta_3,\zeta_4,\zeta_5,\zeta_6) \;=\; & P_1F(t) + Q_1w^2(t) + \zeta_1\left[Q - \alpha_0(C-C_0) + \mu N\right] \\ & + \zeta_2\left[\theta(C-C_0) - \theta_0(T-T_0)\right] \\ & + \zeta_3\left[A - dN - \alpha I\right] \\ & + \zeta_4\left[\beta(N-I)I + \lambda(N-I)\frac{F}{m+F} - (\nu+\alpha+d)I\right] \\ & + \zeta_5\left[r(T)F - r_0\frac{F^2}{K(T)} + \phi NF - \phi_0F - \pi_1\mu_1PF\right] \\ & + \zeta_6\left[w(t)F - \mu_0P - \mu_1PF\right], \end{aligned} \tag{6.5}$$

where $\zeta_i's$, $i = 1,2,...,6$, stand for the adjoint variables. Now, the below given set defines the corresponding differential equations for these variables:

$$\begin{aligned} \zeta_1' &= -\frac{\partial H}{\partial C} = \zeta_1\alpha_0 - \zeta_2\theta, \\ \zeta_2' &= -\frac{\partial H}{\partial T} = \zeta_2\theta_0 - \zeta_5\left[r'(T)F + r_0K'(T)\frac{F^2}{K^2(T)}\right], \\ \zeta_3' &= -\frac{\partial H}{\partial N} = -\left[\zeta_1\mu - \zeta_3d + \zeta_4\left(\beta I + \frac{\lambda F}{m+F}\right) + \zeta_5\phi F\right], \\ \zeta_4' &= -\frac{\partial H}{\partial I} = -\left[-\zeta_3\alpha + \zeta_4\left(\beta(N-2I) - \frac{\lambda F}{m+F} - (\nu+\alpha+d)\right)\right], \\ \zeta_5' &= -\frac{\partial H}{\partial F} = -\left[P_1 + \zeta_4(N-I)\frac{\lambda m}{(m+F)^2} + \zeta_5\left(r(T) - \frac{2r_0F}{K(T)} + \phi N - \phi_0 - \pi_1\mu_1P\right) + \zeta_6(w - \mu_1P)\right], \\ \zeta_6' &= -\frac{\partial H}{\partial P} = \zeta_5\pi_1\mu_1F + \zeta_6(\mu_0 + \mu_1F). \end{aligned} \tag{6.6}$$

The transversality conditions are given by $\zeta_i(T_f) = 0$, $i = 1,2,...,6$. The optimal control w^* is determined through the condition $\frac{\partial H}{\partial w} = 0$ at $w = w^*$, valid on the interval $t \in [0,T_f] : 0 \leq w(t) < w^*$.

This leads to the expression $w^* = -\frac{\zeta_6 F}{2Q_1}$ within the interior of the control set. The outcomes are compiled and presented in the subsequent theorem.

Theorem 6. *The optimal control $w^* \in U$ for system* (6.1)*, which minimizes objective functional* (6.2) *in the specified interval $[0, T_f]$, is defined as*

$$w^* = \max\left\{0, \min\left(\frac{-\zeta_6 F}{2Q_1}, w_{\max}\right)\right\}. \tag{6.7}$$

7. Numerical simulation

To verify the analytical results and visualize the dynamic behavior of our model (2.2), we perform numerical simulation by considering the parameter values listed in Table 1, unless stated otherwise. Since the per-capita growth rate and carrying capacity of carriers are assumed as a function of global average temperature as discussed in the modeling process, therefore for performing the numerical simulation, we consider $r(T)$ and $K(T)$ as a linear function of temperature T, such that $r(T) = r_0 + r_1 T$ and $K(T) = K_0 + K_1 T$, satisfying the conditions $r(0) > 0$, $\frac{dr}{dT} > 0$ and $K(0) > 0$ $\frac{dK}{dT} > 0$, respectively.

Table 1. Values of the parameters used in model system (2.2).

Parameter	Unit	Value	Parameter	Unit	Value
Q	ppm day^{-1}	0.05	θ_0	day^{-1}	0.01
A	persons day^{-1}	100	μ	ppm persons^{-1}day^{-1}	0.0008
K_0	flies	1000	ϕ	persons^{-1}day^{-1}	0.00002
K_1	flies $^\circ C^{-1}$	50	ϕ_0	day^{-1}	0.04
d	day^{-1}	0.01	r_0	day^{-1}	0.05
m	flies	2000	r_1	day^{-1} $^\circ C^{-1}$	0.0001
α_0	day^{-1}	0.0125	π_1	flies kg^{-1}	1
α	day^{-1}	0.2	μ_0	day^{-1}	0.0002
λ	day^{-1}	0.02	μ_2	kg flies^{-1} day^{-1}	0.03
β	persons^{-1}day^{-1}	0.00001	μ_1	flies^{-1} day^{-1}	0.00004
ν	day^{-1}	0.02	C_0	ppm	280
θ	$^\circ C$ ppm^{-1} day^{-1}	0.0005	T_0	$^\circ C$	15

Now, at the parameter values, given in Table 1, the calculated value of the basic reproduction number (R_0) is 0.4347, which is less than unity; and the equilibrium E^* of the system (2.2) is evaluated as:

$$C^* = 555.16,\ T^* = 28.76,\ N^* = 4236.87,\ I^* = 288.16,\ F^* = 4560.24,\ P^* = 749.18.$$

On evaluating the eigenvalues of the Jacobian matrix at the interior equilibrium E^*, we get six negative eigenvalues as -0.03736, -0.08158, -0.1926, -0.1826, $-0.0109 \pm 0.0032i$, which are either negative or possess negative real parts. Thus, the interior equilibrium (E^*) is locally asymptotically stable. Moreover, to visualize the global stability of E^*, we plot the solution trajectories of model system (2.2) in the N-I-F and I-F-P spaces with different initial conditions that lie in the basin of attraction. The resulting solution trajectories consistently converge toward the

equilibrium point (E^*), confirming that (E^*) is globally asymptotically stable, as illustrated in Figure 1.

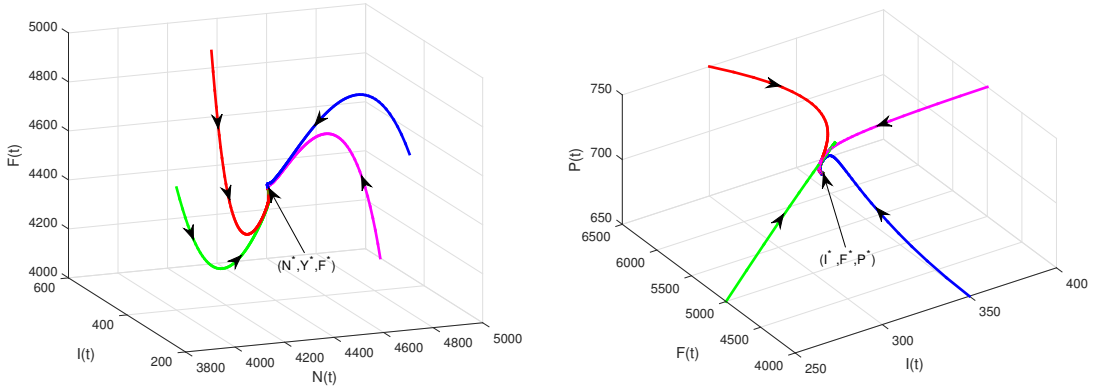

(a) (b)

Figure 1. Nonlinear stability plot of interior equilibrium E^* in (a) *N-I-F* and (b) *I-F-P* spaces.

A bifurcation diagram for the equilibrium level of densities of the infected human population ($I(t)$) and total human population ($N(t)$), corresponding to the basic reproduction number (R_0), is portrayed in Figure 2(a),(b), respectively, which highlight the stability behavior of the disease-free equilibrium. In this figure, the stability of DFE E_0 is displayed with a solid blue line and instability of E_0 is displayed with dashed red lines. Here, we can clearly demonstrate that for $R_0 < 1$, the system possesses a stable disease-free equilibrium, where infections die out in the absence of carriers. At $R_0 = 1$, the transition in the stability behavior occurs and as the basic reproduction number crosses the critical threshold R_0, i.e., for $R_0 > 1$, the transcritical bifurcation occurs and the disease-free equilibrium becomes unstable. Here, it may be noted that for $R_0 > 1$, E_0 becomes unstable, and the carrier-free equilibrium (E_1) emerges, which is always unstable.

In Figure 3(a),(b), we display the contour plots to visualize the dependency of the basic reproduction number (R_0) on the different pairs of parameter values. These contour plots provide insights into how the change in the different parameters promote or control the proliferation of infectious disease, illustrating the conditions under which the infection might persist or die out. Figure 3(a) portrays the change in the value of the basic reproduction number (R_0) corresponding to the immigration rate of susceptible individuals (A) and the disease transmission rate from infected to susceptible individuals through direct contact (β). The low values of A and β result in a low value of R_0. Increasing either A (at the fixed value of β) or β (at the fixed value of A) leads to a higher R_0. Moreover, Figure 3(b) is plotted for visualizing the change in R_0 corresponding to disease transmission rate (β) and disease-induced death rate of infected individuals (α). Here, increasing the value of β leads to an increase in R_0, while increasing α reduces it.

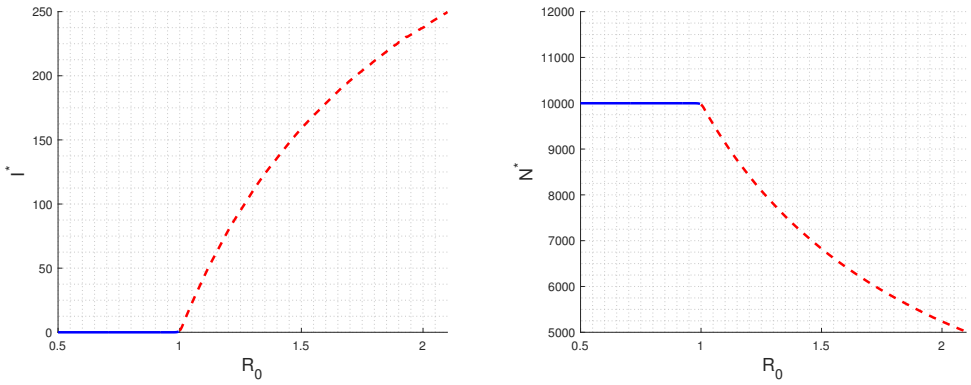

(a) (b)

Figure 2. Bifurcation diagram for the equilibrium level of the densities of (a) infected individuals and (b) total human population corresponding to the basic reproduction number (R_0) at the listed parameter values given in Table 1.

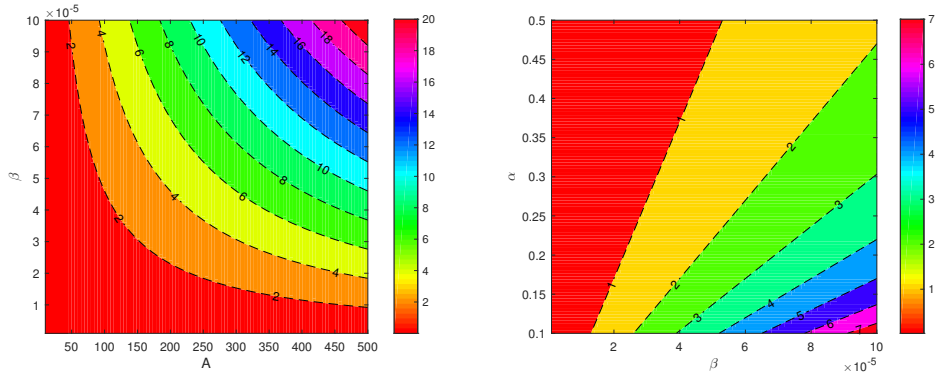

(a) (b)

Figure 3. Contour plots of the basic reproduction number R_0 corresponding to the parameters (a) A and β, (b) β and α, at the listed parameter values given in Table 1.

Further, Figure 4(a),(b) is displayed to illustrate the variations in the densities of the infected population ($I(t)$) and carrier population ($F(t)$), respectively, for the increasing values of per-capita growth rate of the carrier population caused by temperature rise. On increasing the growth rate of the carriers (which is elevated due to the global average temperature) with setting $r_1 = \{0.001, 0.003, 0.005\}$, the values of $I(t)$ and $F(t)$ increase. Similarly, Figure 5(a),(b) illustrates the variations in $I(t)$ and $F(t)$ corresponding to the carrying capacity of carriers (which is elevated due to the global average temperature) with setting $K_1 = \{50, 60, 70\}$. The plot displays the enhanced values of $I(t)$ and $F(t)$ with the increase in K_1. Thus, raising the global average temperature amplifies the spread and persistence of infectious diseases by enhancing the growth and sustainability of carriers, and thus the infected population.

Proceeding further, in Figure 6(a),(b), surface plots are generated to visualize the equilibrium

values of the population densities of infected individuals (I^*) and carriers (F^*) for the varying introduction rate of chemical insecticides to control the carrier population (μ_2) and growth rate of the carrier population because of anthropogenic activities (ϕ). Here, the higher values of I^* and F^* are attained at the low value of μ_2 and high value of ϕ, whereas the lower values of I^* and F^* are attained at the high value of μ_2 and low value of ϕ. These observations highlight the critical balance between the control strategy and environmental factors in managing infectious disease dynamics. This physically signifies that how intensifying the control measures (application of chemical insecticides) or mitigating anthropogenic activities that favor carrier growth can significantly reduce the carrier population, and thus the infected population.

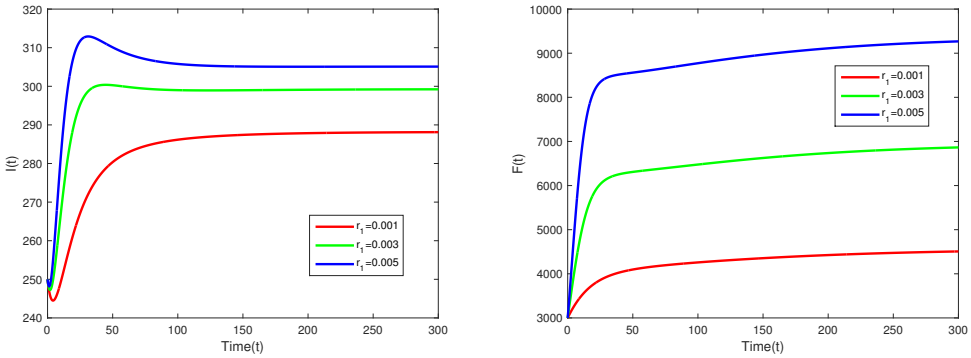

(a) (b)

Figure 4. Variation plot for the densities of infected individuals $I(t)$ and the carrier population $F(t)$ for increasing values of the intrinsic growth rate of the carrier's population elevated by global average temperature (r_1).

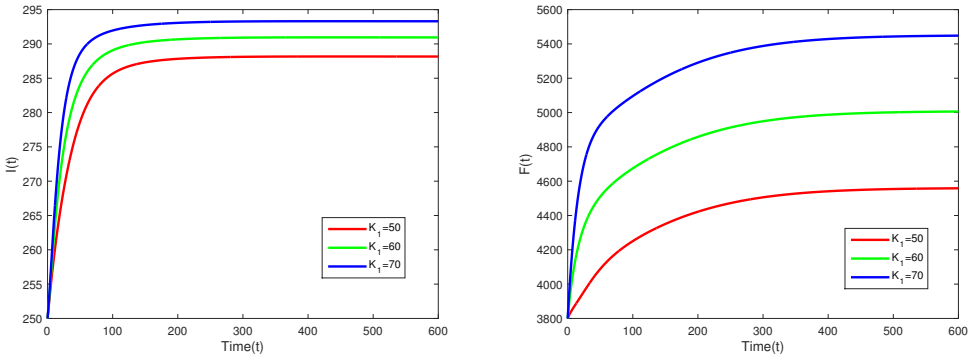

(a) (b)

Figure 5. Variation of densities of infected individuals $I(t)$ and the carrier population $F(t)$ for different values of the carrier density elevated by global average temperature K_1.

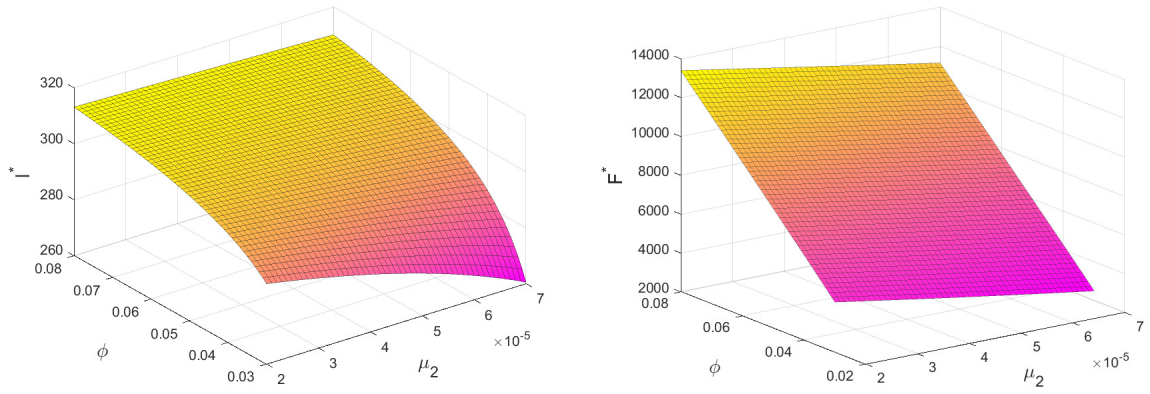

(a) (b)

Figure 6. Surface plots of the equilibrium level of densities of the (a) infected population and (b) carrier population on varying parameters ϕ and μ_2.

7.1. Sensitivity analysis

Sensitivity analysis is used to understand how variations in input parameters affect the solution of model (2.2). In the case of the basic reproduction number (R_0), its normalized forward sensitivity indices quantify the sensitivity of R_0 for variations in each parameter [50].

The following formula is used to calculate these indices as a relative shift in R_0 with respect to a relative shift in parameter (p):

$$S_p = \frac{\partial R_0}{\partial p} \cdot \frac{p}{R_0}.$$

The process involves identifying the system parameters, calculating the partial derivative of R_0 with respect to each parameter, and then normalizing the result to allow comparison. A positive sensitivity index means R_0 increases with the parameter, while a negative index indicates a decrease. The magnitude of the index shows the strength of the parameter's effect on R_0. This analysis helps in determining which parameters are most influential, aiding in decisions about control measures or interventions.

Figure 7 shows that the normalized forward sensitivity indices associated with the basic reproduction number (R_0) exhibit different behaviors. The indices with respect to β and A are both equal to 1, meaning that R_0 increases proportionally to an increase in these parameters. In contrast, the sensitivity indices corresponding to the recovery rate (ν) and disease-induced mortality rate (α) are negative, indicating that an increase in either ν or α decreases R_0. Specifically, the magnitude of these negative indices depends on the ratio of the respective parameter to the sum ($\nu + \alpha + d$), showing that as these death/ recovery rates increase, their influence on reducing R_0 becomes stronger. The index for d is also negative and more complex, with a value less than -1, indicating that increases in d (natural death rate) have a stronger dampening effect on R_0 due to the additional term involving d. Overall, R_0 is the most sensitive to changes in β and A, but increase in d, ν, or α significantly reduces its values as listed in Table 2.

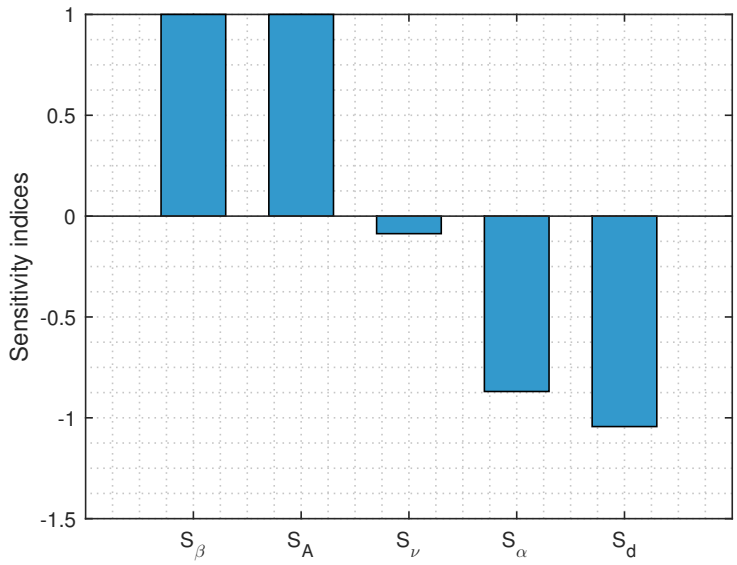

Figure 7. The normalized forward sensitivity indices of R_0 with respect to the listed parameters in Table 2, at the parameter values given in Table 1.

Table 2. Sensitivity indices of the basic reproduction number (R_0).

Parameter	Sensitivity index	Value
β	S_β	+1
A	S_A	+1
ν	S_ν	-0.0870
α	S_α	-0.8696
d	S_d	-1.0435

Global sensitivity analysis (GSA) is used to quantify how uncertainty in model parameters affects the output by exploring the entire input space. Latin hypercube sampling (LHS) efficiently samples the parameter space by dividing each parameter's range into equal intervals and ensuring all portions are represented, allowing for a broad and uniform exploration of parameter values. Partial rank correlation coefficients (PRCC) then measure the correlation between each parameter and model output, controlling for the influence of other parameters and accounting for non-linear relationships. This method isolates the impact of each parameter on the output while considering interactions between parameters. By combining LHS and PRCC, one can determine which parameters significantly influence the model's behavior, helping to manage uncertainty and improve the robustness of simulations, particularly for complex systems where parameters are uncertain or experimentally derived. LHS indeed allows for the simultaneous and efficient sampling of multiple parameters, capturing their interactions in the model, while PRCC provide a measure of correlation between those parameters and the infected and carrier population as a response function, with values ranging from -0.6 (perfect negative correlation) to +1 (perfect positive correlation) and -0.8 to +1. This combination enhances the understanding of how different parameters influence model outcomes.

The magnitude of the PRCC value, regardless of the sign, shows the strength of the correlation. A value close to 1 (or -1) depicts a strong correlation, indicating that the parameter has a significant impact on the output, either positively or negatively. A PRCC value near 0 implies a weak or negligible influence, meaning the parameter has little effect on the output. PRCC help to identify not just which parameters affect the model's output, but also whether their effects are strong or weak, and in what direction they push the system's behavior. This is crucial for prioritizing parameter estimation efforts and improving model accuracy. We have conducted 1000 simulations using Latin hypercube sampling (LHS), assigning uniform distributions to each key parameter. The parameters baseline values are sourced from Table 1, and we allowed for deviations of ± 25% around these values to account for variability and uncertainty. This approach ensures that the parameter space is well-explored while reflecting realistic uncertainty levels. After running the simulations, we calculated the PRCC to estimate the effect of each parameter on the system's output.

The resulting PRCC values, which indicate both the direction and strength of these influences, are visualized as bar graphs in Figures 8 and 9. These graphs provide a clear visual representation of which parameters have the most significant impact on the dynamic variables I and F, helping to focus attention on those with the greatest influence. In Figure 8, it is observed that the model parameters A, β, λ, r_1, K_1, ϕ, θ, and μ demonstrate positive associations with the infected individuals under the epidemic region, suggesting that an increase in these parameters results in the increase of the infected population. This figure further illustrates that the infected population has a negative correlation with the parameters m, ϕ_0, α_0, μ_2, and μ_1, meaning that increasing these parameters can reduce the infected population. Similarly, in Figure 9, we find that parameters A, β, m, r_1, K_1, ϕ, θ, and μ have positive correlations with the carrier population, while λ, ϕ_0, α_0, μ_2, and μ_1 exhibit negative correlations with the carrier population. These sensitivity results suggest that increasing the parameters with negative PRCC values can help to reduce both the infected and carrier population, potentially lowering the epidemic burden.

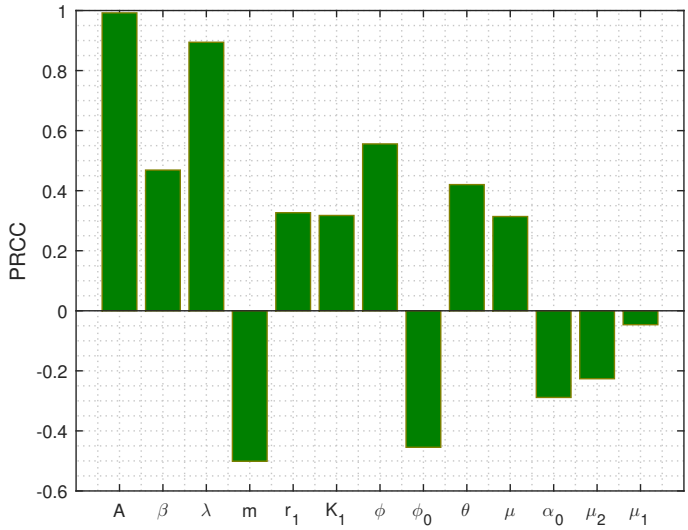

Figure 8. PRCC of parameter values with infected population (I) as the response function.

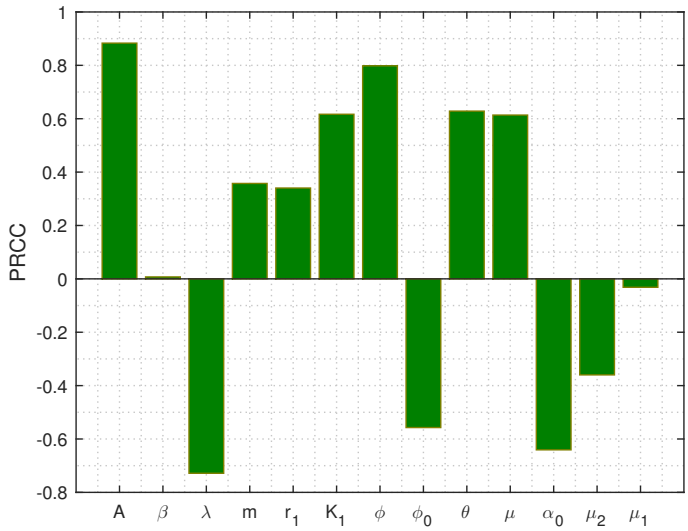

Figure 9. PRCC of parameter values with the carrier population (F) as the response function.

Here, it is worth noting that the parameter d represents the natural death rate of the human population, encompassing both infected and susceptible individuals. A graph illustrating the normalized forward sensitivity indices of the basic reproduction number (R_0) with respect to various parameters, including d has already been provided in Figure 7. Therefore, we chose not to include d, in these PRCC graphs, as natural death is beyond human control. Its influence, whether positive or negative, on the infected and carrier populations, does not offer actionable insights for managing or controlling the proliferation of the infectious disease.

7.2. Optimal control results

Here, the forward-backward sweep approach is used to numerically solve the optimal control problem and quantify the effectiveness of control strategies in mitigating carrier-dependent infectious diseases [49]. This method is widely used as an iterative procedure for optimal control problems that provides a robust framework for finding the optimal strategy to minimize disease prevalence while accounting for intervention costs. The procedure starts with an initial estimate for the control variable, which can represent strategies such as chemical control targeting carriers or other intervention measures aimed at reducing disease transmission. The state variables, infected human population and carrier population, are integrated forward in time by applying the highly accurate fourth-order Runge-Kutta method. In parallel, the system of adjoint (co-state) variables, which reflects the sensitivity of the objective function to variations in state variables, is computed backward in time. In each iteration, the control variable is updated based on the adjoint variables and the gradient of the objective function, ensuring that the intervention strategy moves toward an optimal solution. The forward-backward sweep method is repeated iteratively until convergence is achieved, i.e., when the changes in the control variable become sufficiently small between iterations. We set the weight factors for minimizing both the carrier population and the use of chemical insecticides to $P_1 = Q_1 = 1$, with a maximum control rate of $w_{\max} = 1$. The remaining parameters are consistent with those given in

Table 1. The simulation results, depicted in Figure 10(a),(b), compare the infected and carrier population under the time-dependent optimal control ($w(t)$) and without any control measure. Figure 10(c) clearly demonstrates that the optimal strategy involves applying chemical insecticides at the maximum rate during the first 10 days, and then gradually decreases thereafter. Thus, varying P_1 and Q_1 allows for tailoring the control strategy based on specific priorities, whether it is aggressively reducing the disease spread through carrier elimination or focusing on minimizing intervention costs and side effects. This flexibility enables a more customized approach to disease control in different scenarios. This also aligns with a real-world scenario that the growth time of egg to adult is approximately 7 to 10 days. Therefore, the insecticides are often used during the carrier's peak activity or life cycle stages (when larvae or adult carriers are present) for optimal efficacy of the chemical insecticides, and thus for the control of infectious diseases.

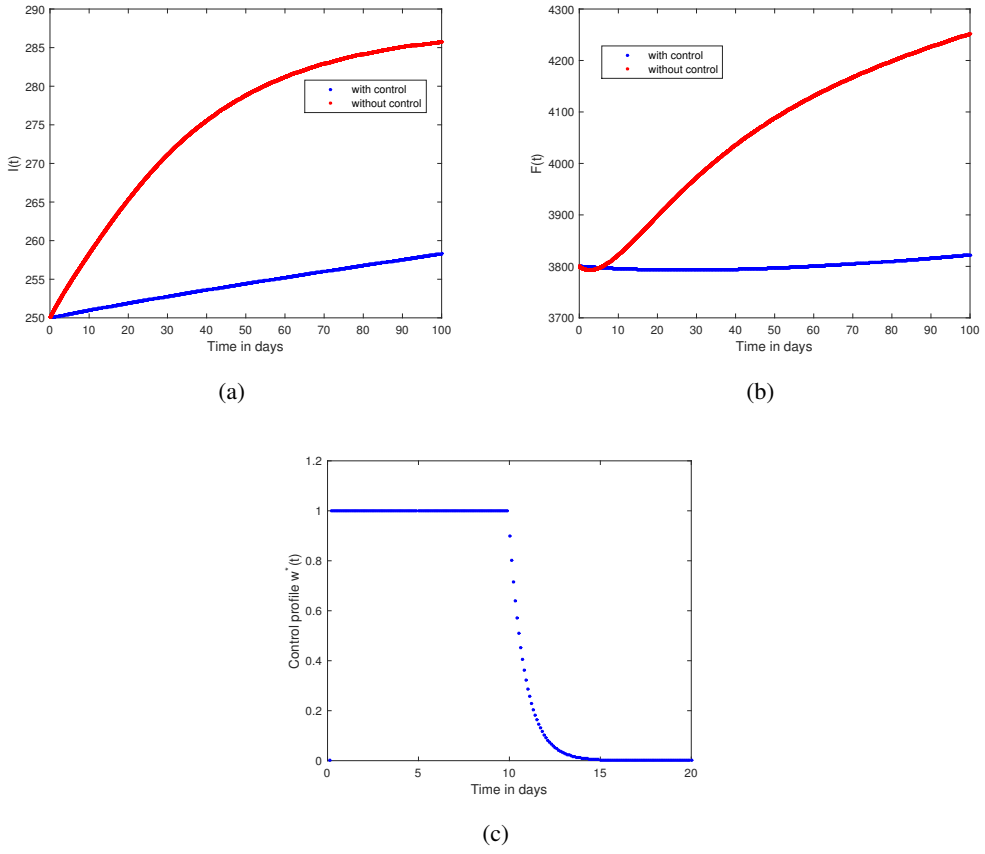

Figure 10. Variation with and without optimal control on the (a) infected population, (b) carrier population, and (c) control profile $w^*(t)$.

8. Conclusions

The world is facing the escalating challenge of climate change with the rising level of atmospheric carbon dioxide and global average temperature, creating favorable conditions for carriers, like houseflies, to thrive and increase their population. These carriers transmit diseases such as

Salmonellosis and Typhoid fever, posing a serious risk to human health. The anthropogenic activities also create the conditions to expand the habitat of carriers and enhance the chances for the proliferation of the infectious disease. This study introduces a mathematical model incorporating an optimal control strategy to examine the impact of chemical insecticides on the dynamics of infectious diseases dependent on carriers. The model includes key parameters, such as the transmission rate, the growth rate of carriers due to human-related activities, and the introduction rate of chemical spraying to control the carrier population, etc. The analysis reveals that a transcritical bifurcation occurs, indicating a threshold value where the basic reproduction number changes stability between the disease-free equilibrium and carrier-free equilibrium. The combined impact of chemical insecticides for controlling the density of carriers and growth rate of the carrier population on the densities of infected individuals and carriers highlight the balance between the control strategy and environmental factors in managing infectious diseases. The results show that by intensifying the control measure (application of chemical insecticides) and mitigating anthropogenic activities that favor carrier growth collectively reduce the carrier population, and thus the infected population. Normalized sensitivity analysis and PRCC identify the most effective parameters, providing insight into their contributions to R_0. Sensitivity analysis using LHS and PRCC identified the most influential parameters affecting the dynamics of the infected and carrier populations. This analysis enables targeted interventions and efficient resource allocation in disease control. The immigration rate and transmission rate via carriers are found to have the greatest impact on the infected population, while the immigration rate and carrier growth due to human-related activities are identified as having the greatest impact on the carrier population. Additionally, we also identify the optimal time for spraying the chemical insecticides to reduce the carriers and thus the proliferation of infectious diseases, which leads to minimizing the carrier density as well as the associated spraying cost. The optimal spraying period lasts about 10 days and should be administered during the developmental stages of the carriers.

Thus, this study underscores the need for a balanced and strategic approach to the use of insecticides as a control strategy in managing carrier-dependent infectious diseases. Also, this study emphasizes the need for reduction of the anthropogenic activities which promote the growth of carriers and distribution of the disease.

Use of AI tools declaration

The authors declare they have not used Artificial Intelligence (AI) tools in the creation of this article.

Acknowledgments

Shubham Chaudhry gratefully acknowledges the financial support provided by CSIR, Government of India, in the form of a Senior Research Fellowship (File No. 08/0078(13682)/2022-EMR-I). Gauri Agrawal is thankful to the Department of Science and Technology, Government of India, for providing financial support in the form of a Senior Research Fellowship (DST/INSPIRE Fellowship/2020/IF200224).

Conflict of interest

Maia Martcheva is a guest editor for [Mathematical Biosciences and Engineering] and was not involved in the editorial review or the decision to publish this article. The authors declare there is no conflict of interest.

References

1. S. Bansal, L. A. Meyers, The impact of past epidemics on future disease dynamics, *J. Theor. Biol.*, **309** (2012), 176–184. https://doi.org/10.1016/j.jtbi.2012.06.012
2. V. J. Cirillo, "Winged Sponges": Houseflies as carriers of typhoid fever in 19th- and early 20th-century military camps, *Perspect. Biol. Med.*, **49** (2006), 52–63. https://doi.org/10.1353/pbm.2006.0005
3. B. Chala, F. Hamde, Emerging and re-emerging vector-borne infectious diseases and the challenges for control: A review, *Front. Public Health*, **9** (2021), 715759. https://doi.org/10.3389/fpubh.2021.715759
4. A. Flahault, R. R. de Castaneda, I. Bolon, Climate change and infectious diseases, *Public Health Rev.*, **37** (2016), 21. https://doi.org/10.1186/s40985-016-0035-2
5. B. Traore, O. Koutou, B. Sangare, A global mathematical model of malaria transmission dynamics with structured mosquito population and temperature variations, *Nonlinear Anal. Real World Appl.*, **53** (2020), 103081. https://doi.org/10.1016/j.nonrwa.2019.103081
6. L. J. Nunes, The rising threat of atmospheric CO_2: A review on the causes, impacts, and mitigation strategies, *Environments*, **10** (2023), 66. https://doi.org/10.3390/environments10040066
7. N. P. Gillett, M. Kirchmeier-Young, A. Ribes, H. Shiogama, G. C. Hegerl, R. Knutti, et al., Constraining human contributions to observed warming since the pre-industrial period, *Nat. Clim. Change*, **11** (2021), 207–212. https://doi.org/10.1038/s41558-020-00965-9
8. M. Baylis, Potential impact of climate change on emerging vector-borne and other infections in the UK, *Environ. Health*, **16** (2017), 112. https://doi.org/10.1186/s12940-017-0326-1
9. S. Bahrndorff, A. Ruiz-Gonzalez, N. De Jonge, J. L. Nielsen, H. Skovgard, C. Pertoldi, Integrated genome-wide investigations of the housefly, a global vector of diseases reveal unique dispersal patterns and bacterial communities across farms, *BMC Genomics*, **21** (2020), 66. https://doi.org/10.1186/s12864-020-6445-z
10. F. M. Chikezie, K. N. Opara, P. M. E. Ubulom, Impacts of changing climate on arthropod vectors and diseases transmission, *Niger. J. Entomol.*, **40** (2024), 179–192. https://doi.org/10.36108/NJE/4202/04.0161
11. L. Francuski, W. Jansen, L. W. Beukeboom, Effect of temperature on egg production in the common housefly, *Entomol. Exp. Appl.*, **168** (2020), 513–522. https://doi.org/10.1111/eea.12912
12. P. J. Edelson, R. Harold, J. Ackelsberg, J. S. Duchin , S. J. Lawrence , Y. C. Manabe, et al., Climate change and the epidemiology of infectious diseases in the United States, *Clin. Infect. Dis.*, **76** (2023), 950–956. https://doi.org/10.1093/cid/ciac697

13. H. Skovgard, G. Nachman, Temperature-and age-dependent survival, development, and oviposition rates of the pupal parasitoid spalangia cameroni (Hymenoptera: Pteromalidae), *Environ. Entomol.*, **45** (2016), 1063–1075. https://doi.org/10.1093/ee/nvw055

14. C. J. Geden, H. Biale, E. Chiel, D. M. Johnson, Effect of fluctuating high temperatures on house flies (Diptera: Muscidae) and their principal parasitoids (Muscidifurax spp. and Spalangia spp. [Hymenoptera: Pteromalidae]) from the United States, *J. Med. Entomol.*, **56** (2019), 1650–1660. https://doi.org/10.1093/jme/tjz080

15. R. W. Sutherst, Global change and human vulnerability to vector-borne diseases, *Clin. Microbiol. Rev.*, **17** (2004), 136–173. https://doi.org/10.1128/CMR.17.1.136-173.2004

16. C. Caminade, K. M. McIntyre, A. E. Jones, Impact of recent and future climate change on vector-borne diseases, *Ann. N. Y. Acad. Sci.*, **1436** (2019), 157–173. https://doi.org/10.1111/nyas.13950

17. H. Van Den Berg, M. Zaim, R. S. Yadav, A. Soares, B. Ameneshewa, A. Mnzava, et al., Global trends in the use of insecticides to control vector-borne diseases, *Environ. Health Perspect.*, **120** (2012), 577–582. https://doi.org/10.1289/ehp.1104340

18. H. Van Den Berg, R. Velayudhan, R. S. Yadav, Management of insecticides for use in disease vector control: Lessons from six countries in Asia and the Middle East, *PLoS Negl. Trop. Dis.*, **15** (2021), e0009358. https://doi.org/10.1371/journal.pntd.0009358

19. A. M. Mohanrao, Extension guidelines for pest/vector management in human habitations, *MANAGE*, (2019). Available from: https://nirdpr.org.in/nird_docs/other/Extension_guidelines_Pests_Rodents_Management.pdf.

20. N. C. Hinkle, J. A. Hogsette, A review of alternative controls for house flies, *Insects*, **12** (2021), 1042. https://doi.org/10.3390/insects12111042

21. K. Karunamoorthi, S. Sabesan, Insecticide resistance in insect vectors of disease with special reference to mosquitoes: A potential threat to global public health, *Health Scope*, **2** (2013), 4–18. https://doi.org/10.17795/jhealthscope-9840

22. M. Ghosh, P. Chandra, P. Sinha, J. B. Shukla, Modelling the spread of carrier-dependent infectious diseases with environmental effect, *Appl. Math. Comput.*, **152** (2004), 385–402. https://doi.org/10.1016/S0096-3003(03)00564-2

23. P. Das, D. Mukherjee, A. K. Sarkar, Study of a carrier dependent infectious disease-cholera, *J. Biol. Syst.*, **13** (2005), 233–244. https://doi.org/10.1142/S0218339005001495

24. R. Naresh, S. Pandey, A. K. K. Misra, Analysis of a vaccination model for carrier dependent infectious diseases with environmental effects, *Nonlinear Anal.: Model. Control*, **13** (2008), 331–350. https://doi.org/10.15388/NA.2008.13.3.14561

25. X. Z. Li, W. S. Li, M. Ghosh, Stability and bifurcation of an SIS epidemic model with treatment, *Chaos, Solitons Fractals*, **42** (2009), 2822–2832. https://doi.org/10.1016/j.chaos.2009.04.024

26. D. Kalajdzievska, M. Y. Li, Modeling the effects of carriers on transmission dynamics of infectious diseases, *Math. Biosci. Eng.*, **8** (2011), 711–722. https://doi.org/10.3934/mbe.2011.8.711

27. J. B. Shukla, V. Singh, A. K. Misra, Modeling the spread of an infectious disease with bacteria and carriers in the environment, *Nonlinear Anal. Real World Appl.*, **12** (2011), 2541–2551. https://doi.org/10.1016/j.nonrwa.2011.03.003

28. A. K. Misra, V. Singh, A delay mathematical model for the spread and control of water borne diseases, *J. Theor. Biol.*, **301** (2012), 49–56. https://doi.org/10.1016/j.jtbi.2012.02.006
29. R. K. Gupta, R. K. Rai, P. K. Tiwari, A. K. Misra, M. Martcheva, A mathematical model for the impact of disinfectants on the control of bacterial diseases, *J. Biol. Dyn.*, **17** (2023), 2206859. https://doi.org/10.1080/17513758.2023.2206859
30. D. Bolatova, S. Kadyrov, A. Kashkynbayev, Mathematical modeling of infectious diseases and the impact of vaccination strategies, *Math. Biosci. Eng.*, **21** (2024), 7103–7123. https://doi.org/10.3934/mbe.2024314
31. A. K. Misra, A. Gupta, E. Venturino, Modeling biological control of carrier-dependent infectious diseases, *Comput. Math. Methods*, **3** (2021), e1127. https://doi.org/10.1002/cmm4.1127
32. L. Liu, X. Wang, Y. Li, Mathematical analysis and optimal control of an epidemic model with vaccination and different infectivity, *Math. Biosci. Eng.*, **20** (2023), 20914–20938. https://doi.org/10.3934/mbe.2023925
33. R. Naresh, S. R. Verma, J. B. Shukla, M. Agarwal, Modeling the effect of sanitation effort on the spread of carrier-dependent infectious diseases due to environmental degradation, *Appl. Appl. Math.*, **18** (2023).
34. S. Singh, P. Chandra, J. B. Shukla, Modeling and analysis of the spread of carrier dependent infectious diseases with environmental effects, *J. Biol. Syst.*, **11** (2003), 325–335. https://doi.org/10.1142/S0218339003000877
35. A. K. Misra, S. N. Mishra, A. L. Pathak, P. K. Srivastava, P. Chandra, A mathematical model for the control of carrier-dependent infectious diseases with direct transmission and time delay, *Chaos, Solitons Fractals*, **57** (2013), 41–53. https://doi.org/10.1016/j.chaos.2013.08.002
36. K. Lata, S. N. Mishra, A. K. Misra, An optimal control problem for carrier dependent diseases, *Biosystems*, **187** (2020) 104039. https://doi.org/10.1016/j.biosystems.2019.104039
37. A. K. Misra, A. Jha, Modeling the effect of population pressure on the dynamics of carbon dioxide gas, *J. Appl. Math. Comput.*, **67** (2021), 623–640. https://doi.org/10.1007/s12190-020-01492-8
38. J. K. Hale, *Ordinary Differential Equations*, Wiley–Interscience, 1969.
39. H. I. Freedman, J. W. H. So, Global stability and persistence of simple food chains, *Math. Bio.*, **76** (1985), 69–86. https://doi.org/10.1016/0025-5564(85)90047-1
40. G. Agrawal, A. K. Agrawal, J. Dhar, A. K. Misra, Modeling the impact of cloud seeding to rescind the effect of atmospheric pollutants on natural rainfall, *Model. Earth Syst. Environ.*, **10** (2024), 1573–1588. https://doi.org/10.1007/s40808-023-01854-8
41. G. Agrawal, A. K. Agrawal, J. Dhar, Effects of human population and atmospheric pollution on rainfall: A modeling study, *J. Indian Math. Soc.*, **91** (2024), 550–564.
42. G. Agrawal, A. K. Agrawal, A. K. Misra, Modeling the impacts of chemical substances and time delay to mitigate regional atmospheric pollutants and enhance rainfall, *Phys. D: Nonlinear Phenom.*, **472** (2025), 134507. https://doi.org/10.1016/j.physd.2024.134507
43. T. K. Kar, A. Batabyal, Stability analysis and optimal control of an SIR epidemic model with vaccination, *Biosystems*, **104** (2011), 127–135. https://doi.org/10.1016/j.biosystems.2011.02.001

44. T. K. Kar, S. Jana, A theoretical study on mathematical modelling of an infectious disease with application of optimal control, *Biosystems*, **111** (2013), 37–50. https://doi.org/10.1016/j.biosystems.2012.10.003

45. S. Singh, Modeling the effect of global warming on the spread of carrier dependent infectious diseases, *Model. Earth Syst. Environ.*, **3** (2017), 39. https://doi.org/10.1007/s40808-017-0292-1

46. D. L. Lukes, *Differential Equations: Classical to Control*, Academic Press, 1982.

47. W. H. Fleming, R. W. Rishel, *Deterministic and Stochastic Optimal Control*, Springer-Verlag, 1975.

48. L. S. Pontryagin, V. G. Boltyanskii, R. V. Gamkrelidze, E. F. Mishchenko, *The Mathematical Theory of Optimal Processes*, Wiley, 1962.

49. S. Lenhart, J. T. Workman, *Optimal Control Applied to Biological Models*, CRC Press, 2007. https://doi.org/10.1201/9781420011418

50. M. Martcheva, *An Introduction to Mathematical Epidemiology*, Springer, 2015. https://doi.org/10.1007/978-1-4899-7612-3

AIMS Press